A REDUCED MODEL FOR INTERNAL WAVES INTERACTING WITH TOPOGRAPHY AT INTERMEDIATE DEPTH *

AILÍN RUIZ DE ZÁRATE† AND ANDRÉ NACHBIN‡

Abstract.
A reduced one-dimensional strongly nonlinear model for the evolution of internal waves over an arbitrary bottom topography is derived. The reduced model is aimed at obtaining an efficient numerical method for the two-dimensional problem. Two layers containing inviscid, immiscible, irrotational fluids of different densities are defined. The upper layer is shallow compared with the characteristic wavelength at the interface of the two-fluid system, while the bottom region's depth is comparable to the characteristic wavelength. The nonlinear evolution equations obtained describe the behaviour of the internal wave elevation and mean upper-velocity for this water configuration. The system is a generalization of the one proposed by Choi and Camassa for the flat bottom case in the same physical settings. Due to the presence of topography a variable coefficient accompanies each space derivative. These Boussinesq-type equations contain the Intermediate Long Wave (ILW) equation and the Benjamin-Ono (BO) equation when restricted to the unidirectional wave regime. We intend to use this model to study the interaction of waves with the bottom profile. The dynamics include wave scattering, dispersion and attenuation among other phenomena.

Key words. Internal waves, Inhomogeneous media, Asymptotic theory.
AMS subject classifications. 76B55, 76B15, 76B07, 35Q35.

1. Introduction

Modelling internal waves is of great interest in the study of ocean and atmosphere dynamics. Internal ocean waves, for example, appear when salt concentration and differences in temperature generate stratification. They can interact with the bottom topography and submerged structures as well as surface waves. In particular, in oil recovery in deep ocean waters, internal waves can affect offshore operations and submerged structures. Another example in the context of atmosphere dynamics is the effect of the form drag of the topography (such as an urban area) which is of importance in the study of polution dispersion. The understanding of the impact of the orography as well as smaller topographic features on the atmosphere can lead to a significant improvement in weather forecasting. Accurate reduced models are a first step in producing efficient computational methods in engineering problems in oceanography and meteorology. This was the goal in [24, 1].

To describe this nonlinear wave phenomenon in deep waters there are several bidirectional models containing the Intermediate Long Wave (ILW) equation and the Benjamin-Ono (BO) equation, starting from works such as [2, 8, 26, 16, 18] to more recent papers such as [20, 5, 6, 7, 15]. The aforementioned bidirectional models consider flat or slowly varying bottom topography. In this paper the model of Choi and Camassa is generalized to the case of an arbitrary bottom topography by using the conformal mapping technique described in [24]. We obtained a strongly nonlinear long-wave model like Choi and Camassa's which is able to describe large amplitude internal solitary waves. A system of two layers constrained to a region limited by a horizontal rigid lid at the top and an arbitrary bottom topography is considered, as

*
†Instituto de Matemática Pura e Aplicada, Estrada Dona Castorina 110, Jardim Botânico, Rio de Janeiro, RJ, Brazil, CEP 22460-320 (ailin@impa.br). The author was supported by an ANP/PRH-32 scholarship.

‡Instituto de Matemática Pura e Aplicada, Estrada Dona Castorina 110, Jardim Botânico, Rio de Janeiro, RJ, Brazil, CEP 22460-320 (nachbin@impa.br). This work was supported by CNPq/Brazil under Grant 300368/96-8.

described in Fig. 2.1. The upper layer is shallow compared with the characteristic wavelength at the interface of the two-fluid system, while the lower region is deeper. The nonlinear evolution equations describe the behaviour of the internal wave elevation and mean upper-velocity for this water configuration. These Boussinesq-type equations contain the ILW equation and the BO equation in the unidirectional wave regime. We intend to use this model to study the interaction of waves with the bottom profile. The dynamics include wave scattering, dispersion and attenuation among other phenomena.

The paper is organized as follows. In Section 2 the physical setting is presented, along with a set of upper layer averaged equations that will be completed with information provided by the lower layer in order to obtain the reduced model. The continuity of pressure at the interface establishes a connection between both layers. Through this condition we add the topography information to the averaged upper layer system. The case when the depth of the bottom layer approaches infinity is also considered. A brief discussion on numerical modeling appears in Section 3. In Section 4 a variable coefficient ILW equation and the BO equation are obtained from the reduced model as unidirectional wave propagation models. Technical justifications for the manipulations done in Section 4 are provided in Appendix A.

2. Derivation of the equations governing the dynamics

We start with a two-fluid configuration. Define the density of each inviscid, immiscible, irrotational fluid as ρ_1 for the upper fluid and ρ_2 for the lower fluid. For a stable stratification, let $\rho_2 > \rho_1$. Similarly, (u_i, w_i) denotes the velocity components and p_i the pressure, where $i = 1,2$. The upper layer is assumed to have an undisturbed thickness h_1, much smaller than the characteristic wavelength of the perturbed interface $L > 0$, hence the upper layer will be in the shallow water regime. At the lower layer the irregular bottom is described by $z = h_2(h(x/l) - 1)$. The function h does not need to be continuous neither univalued. See for example Fig. 2.1 where a polygonal shaped topography is sketched. We can assume h has compact support so the roughness is confined to a finite interval. Moreover h_2 is the undisturbed thickness of the lower layer outside the irregular bottom region and it is comparable with the characteristic wavelength L, which characterizes an intermediate depth regime. When a rapidly varying bottom is of concern, the horizontal length scale for bottom irregularities l is such that $h_1 < l \ll L$. In the slowly varying bottom case we define $\varepsilon = L/l \ll 1$. The coordinate system is positioned at the undisturbed interface between layers. The displacement of the interface is denoted by $\eta(x,t)$ and we may assume that initially it has compact support. See Fig. 2.1.

The corresponding Euler equations are

$$\begin{aligned} u_{ix} + w_{iz} &= 0, \\ u_{it} + u_i u_{ix} + w_i u_{iz} &= -\frac{p_{ix}}{\rho_i}, \\ w_{it} + u_i w_{ix} + w_i w_{iz} &= -\frac{p_{iz}}{\rho_i} - g, \end{aligned}$$

for $i = 1,2$. Subscripts x, z and t stand for partial derivatives with respect to spatial coordinates and time. The continuity condition at the interface $z = \eta(x,t)$ demands that

$$\eta_t + u_i \eta_x = w_i, \qquad p_1 = p_2,$$

namely, a kinematic condition for the material curve and no pressure jumps allowed.

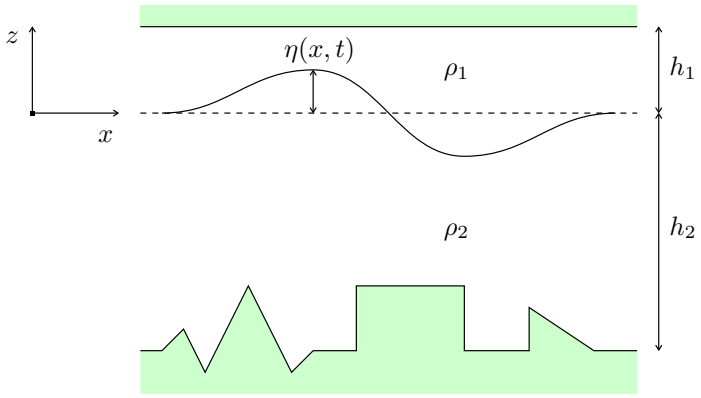

FIG. 2.1. *Two-fluid system configuration.*

At the top we impose a rigid lid condition,

$$w_1(x,h_1,t)=0,$$

commonly used in ocean and atmospheric models, while at the irregular impermeable bottom

$$-\frac{h_2}{l}h'\left(\frac{x}{l}\right)u_2+w_2=0.$$

Introducing the dimensionless dispersion parameter $\beta=\left(\frac{h_1}{L}\right)^2$, it follows from the shallowness of the upper layer that

$$O\left(\sqrt{\beta}\right)=O\left(\frac{h_1}{L}\right)\ll 1.$$

From the continuity equation for $i=1$ we have,

$$\frac{w_1}{u_1}=O\left(\frac{h_1}{L}\right)=O\left(\sqrt{\beta}\right).$$

Let $U_0=\sqrt{gh_1}$ be the characteristic shallow layer speed. According to these scalings, physical variables involved in the upper layer equations are non-dimensionalized as follows:

$$x=L\tilde{x}, \qquad z=h_1\tilde{z}, \qquad t=\frac{L}{U_0}\tilde{t}, \qquad \eta=h_1\tilde{\eta},$$
$$p_1=(\rho_1U_0^2)\tilde{p_1}, \qquad u_1=U_0\tilde{u}_1, \qquad w_1=\sqrt{\beta}U_0\tilde{w}_1.$$

In a weakly nonlinear theory, η is usually scaled by a small parameter. Note that here we have an $O(1)$ scaling. This will lead to a strongly nonlinear model.

2.1. Reducing the upper layer dynamics to the interface

The dimensionless equations for the upper layer (the tilde has been removed) are:

$$u_{1x}+w_{1z}=0,$$
$$u_{1t}+u_1u_{1x}+w_1u_{1z}=-p_{1x},$$
$$\beta(w_{1t}+u_1w_{1x}+w_1w_{1z})=-p_{1z}-1.$$

The boundary conditions are

$$\eta_t + u_1\eta_x = w_1 \quad \text{and} \quad p_1 = p_2 \quad \text{at} \quad z = \eta(x,t), \qquad (2.1)$$
$$w_1(x,1,t) = 0.$$

Focusing on the upper shallow region, consider the following definition: for any function $f(x,z,t)$, let its associated *mean-layer quantity* $\overline{f}$ be

$$\overline{f}(x,t) = \frac{1}{1-\eta}\int_\eta^1 f(x,z,t)\,dz.$$

By averaging we will reduce the two-dimensional (2D) Euler equations to a one-dimensional (1D) system.

Let $\eta_1 = 1-\eta$. From the horizontal momentum equation,

$$\eta_1\overline{u_{1t}} + \eta_1\overline{u_1u_{1x}} + \eta_1\overline{w_1u_{1z}} = -\eta_1\overline{p_{1x}}. \qquad (2.2)$$

We need to express each of these mean-layer quantities in terms of $\overline{u_1}$ and η. The difficulty at this stage is breaking up the mean of square, and other general quadratic terms, into individually averaged terms. Manipulating these mean-layer quantities and using the incompressibility and boundary conditions, we are able to obtain the following three identities:

$$\eta_1\overline{u_{1t}} = \frac{d}{dt}(\eta_1\overline{u_1}) + \eta_t u_1, \qquad (2.3)$$

$$2\eta_1\overline{u_1u_{1x}} = \eta_x u_1^2 + \left(\eta_1\overline{u_1^2}\right)_x, \qquad (2.4)$$

$$\eta_1\overline{w_1u_{1z}} = -w_1u_1 + \frac{1}{2}\eta_x u_1^2 + \frac{1}{2}\left(\eta_1\overline{u_1^2}\right)_x. \qquad (2.5)$$

Substituting Eqs. (2.3), (2.4) and (2.5) in Eq. (2.2) the following mean-layer equation [7] for the upper fluid is derived:

$$(\eta_1\overline{u_1})_t + \left(\eta_1\overline{u_1^2}\right)_x = -\eta_1\overline{p_{1x}}. \qquad (2.6)$$

The incompressibility condition gives $w_1 = \eta_1\overline{u_{1x}}$ at $z = \eta(x,t)$. This, together with the identity

$$\eta_1\overline{u_{1x}} = u_1\eta_x + (\eta_1\overline{u_1})_x,$$

shows that

$$w_1 = u_1\eta_x + (\eta_1\overline{u_1})_x.$$

Substitution of w_1 into Eq. (2.1) leads to $\eta_t + u_1\eta_x = u_1\eta_x + (\eta_1\overline{u_1})_x$ and

$$-\eta_{1t} = (\eta_1\overline{u_1})_x. \qquad (2.7)$$

As pointed out in [7], the system of Eqs. (2.6)–(2.7) was already considered in [28, 4] for surface waves. In reducing (averaging) the 2D Euler equations to this 1D system

no approximations have been made up to this point. Nevertheless, the quantities $\overline{u_1 \cdot u_1}$ and $\overline{p_{1x}}$ prevent the closure of the system of Eqs. (2.6)–(2.7). These quantities will be expressed in terms of η and $\overline{u_1}$ up to a certain order in the dispersion parameter β. Note that until now, we still have not used the vertical momentum equation and the continuity of pressure boundary condition. We start by approximating $\overline{p_{1x}}$ and then follow to do the same for $\overline{u_1 \cdot u_1}$.

The vertical momentum equation over a shallow layer suggests the following asymptotic expansion in powers of β

$$f(x,z,t) = f^{(0)} + \beta f^{(1)} + O(\beta^2)$$

for any of the functions u_1, w_1, p_1. Since $p_{1z} = -1 + O(\beta)$, integration from η to z leads to

$$p_1(x,z,t) - p_1(x,\eta,t) = -(z-\eta) + O(\beta),$$

and the pressure continuity across the interface gives

$$p_1(x,z,t) = p_2(x,\eta,t) - (z-\eta) + O(\beta).$$

Pressure $p_2(x,\eta,t)$ should be non-dimensionalized in the same fashion as p_1, that is,

$$p_2 = \rho_1 U_0^2 \tilde{p}_2.$$

Define $P(x,t) = p_2\big(x,\eta(x,t),t\big)$. Then

$$p_1 = P(x,t) - (z-\eta) + O(\beta),$$

which immediately yields

$$\overline{p_{1x}} = \Big(p_2\big(x,\eta(x,t),t\big) \Big)_x + \eta_x + O(\beta). \tag{2.8}$$

An approximation for P_x will be obtained later from the Euler equations for the lower fluid layer. We now approximate the mean squared horizontal velocity in terms of $\overline{u_1}$ and η.

In order to express $\overline{u_1 \cdot u_1}$ as a function of $\overline{u_1}$ and η, it should be pointed out that the irrotational condition in non-dimensional variables is

$$\frac{U_0}{h_1} u_{1z} = \sqrt{\beta} \frac{U_0}{L} w_{1x},$$

i. e. $u_{1z} = \beta w_{1x}$. Hence $({u_1}^{(0)})_z = 0$ and as expected for shallow water flows $u_1^{(0)}$ is independent from z:

$$u_1^{(0)} = u_1^{(0)}(x,t). \tag{2.9}$$

We now correct this first order approximation. By using

$$u_1 = u_1^{(0)} + \beta u_1^{(1)} + O(\beta^2), \tag{2.10}$$

and Eq. (2.9), it is straightforward that

$$\overline{u_1 \cdot u_1} = u_1^{(0)} \cdot u_1^{(0)} + 2\beta u_1^{(0)} \overline{u_1^{(1)}} + O(\beta^2) \tag{2.11}$$

and

$$\overline{u_1}\cdot\overline{u_1} = u_1^{(0)}\cdot u_1^{(0)} + 2\beta u_1^{(0)}\overline{u_1^{(1)}} + O(\beta^2),$$

thus leading to

$$\eta_1\overline{u_1\cdot u_1} = \eta_1\overline{u_1}\cdot\overline{u_1} + O(\beta^2). \tag{2.12}$$

Using Eq. (2.12) and Eq. (2.7), Eq. (2.6) becomes

$$\eta_1\overline{u_1}_t + \eta_1\overline{u_1}\cdot\overline{u_1}_x = -\eta_1\overline{p_1}_x + O(\beta^2).$$

After substitution of Eq. (2.8), the following set of approximate equations for the upper layer has been deduced from Eqs. (2.6), (2.7):

$$\begin{aligned} -\eta_t + \big((1-\eta)\overline{u_1}\big)_x &= 0, \\ \overline{u_1}_t + \overline{u_1}\cdot\overline{u_1}_x &= -\eta_x - \Big(p_2\big(x,\eta(x,t),t\big)\Big)_x + O(\beta). \end{aligned}$$

We have almost closed our system of PDEs. Now we need to get an expression for p_2 in order to close the system and also establish a connection with the lower intermediate depth layer.

2.2. Connecting the upper and lower layers

The coupling of the upper and lower layers is done through the pressure term. To get an approximation for $P_x(x,t) = \Big(p_2\big(x,\eta(x,t),t\big)\Big)_x$ from the Euler equations for the lower fluid layer, observe that not being in the shallow water configuration we take

$$\frac{h_2}{L} = O(1),$$

so that the following scaling relation

$$\frac{w_2}{u_2} = O\left(\frac{h_2}{L}\right) = O(1)$$

is valid as a consequence of the continuity equation. At the interface, from the continuity of vertical velocities and the relations above, we have that

$$\frac{w_2}{u_1} = O\left(\sqrt{\beta}\right), \qquad \frac{u_2}{u_1} = O\left(\sqrt{\beta}\right),$$

at $z=\eta$. Following these scalings introduce the dimensionless variables for the lower region (with a tilde)

$$\begin{aligned} &x = L\tilde{x}, && z = L\tilde{z}, && t = \frac{L}{U_0}\tilde{t}, && \eta = h_1\tilde{\eta}, \\ &p_2 = (\rho_1 U_0^2)\tilde{p}_2, && u_2 = \sqrt{\beta}U_0\tilde{u}_2, && w_2 = \sqrt{\beta}U_0\tilde{w}_2. \end{aligned}$$

This naturally suggests that we introduce the velocity potencial $\phi = \sqrt{\beta}U_0 L\tilde{\phi}$. Note that the definition for $\tilde{z}$ is different from the one for the upper region, since it involves

the characteristic wavelength L instead of the vertical scale h_2. This is consistent since both scales are of the same order.

In these dimensionless variables, the Bernoulli law for the interface reads

$$\sqrt{\beta}\phi_t+\frac{\beta}{2}\left(\phi_x^2+\phi_z^2\right)+\eta+\frac{\rho_1}{\rho_2}P=\mathcal{C}(t),$$

where the tilde has been ignored. $\mathcal{C}(t)$ is an arbitrary function of time. Then, up to order β, the pressure derivative P_x is

$$P_x=-\frac{\rho_2}{\rho_1}\left(\eta_x+\sqrt{\beta}\phi_t(x,\sqrt{\beta}\eta,t)_x\right)+O(\beta), \tag{2.13}$$

where ϕ satisfies the Neumann problem with an upper free surface boundary, given as

$$\begin{cases}\phi_{xx}+\phi_{zz}=0, & \text{on } -\dfrac{h_2}{L}+\dfrac{h_2h(Lx/l)}{L}\le z\le\sqrt{\beta}\eta(x,t),\\[2ex] \phi_z=\eta_t+\sqrt{\beta}\eta_x\phi_x, & \text{at } z=\sqrt{\beta}\eta(x,t),\\[2ex] -\dfrac{h_2}{l}h'(Lx/l)\phi_x+\phi_z=0, & \text{at } z=-\dfrac{h_2}{L}+\dfrac{h_2h(Lx/l)}{L}.\end{cases} \tag{2.14}$$

Furthermore, Taylor expansion in z gives

$$\begin{aligned}\left[\sqrt{\beta}\phi_t\left(x,\sqrt{\beta}\eta,t\right)\right]_x&=\sqrt{\beta}\phi_{tx}\left(x,\sqrt{\beta}\eta,t\right)+\beta\phi_{tz}\left(x,\sqrt{\beta}\eta,t\right)\eta_x,\\ &=\sqrt{\beta}\phi_{tx}\left(x,\sqrt{\beta}\eta,t\right)+O(\beta),\\ &=\sqrt{\beta}\phi_{tx}(x,0,t)+O(\beta).\end{aligned}$$

Therefore,

$$P_x=-\frac{\rho_2}{\rho_1}\left(\eta_x+\sqrt{\beta}\phi_{tx}(x,0,t)\right)+O(\beta). \tag{2.15}$$

As in the flat bottom case [7], from Eq. (2.15) it is clear that it is sufficient to find the horizontal velocity ϕ_x at $z=0$ in order to obtain P_x at the interface. Due to the presence of the small parameter $\sqrt{\beta}$ in problem (2.14), $\phi_x(x,0,t)$ can be approximated by the horizontal velocity at $z=0$ that comes from the linearized problem around $z=0$:

$$\begin{cases}\phi_{xx}+\phi_{zz}=0, & \text{on } -\dfrac{h_2}{L}+\dfrac{h_2h(Lx/l)}{L}\le z\le 0,\\[2ex] \phi_z=\eta_t, & \text{at } z=0,\\[2ex] -\dfrac{h_2}{l}h'(Lx/l)\phi_x+\phi_z=0, & \text{at } z=-\dfrac{h_2}{L}+\dfrac{h_2h(Lx/l)}{L}.\end{cases} \tag{2.16}$$

In this systematic reduction we use a Taylor expansion to ensure that

$$\begin{aligned}\phi_z(x,0,t)&=\phi_z\left(x,\sqrt{\beta}\eta,t\right)+O\left(\sqrt{\beta}\right),\\ &=\eta_t+\sqrt{\beta}\eta_x\phi_x+O\left(\sqrt{\beta}\right),\end{aligned}$$

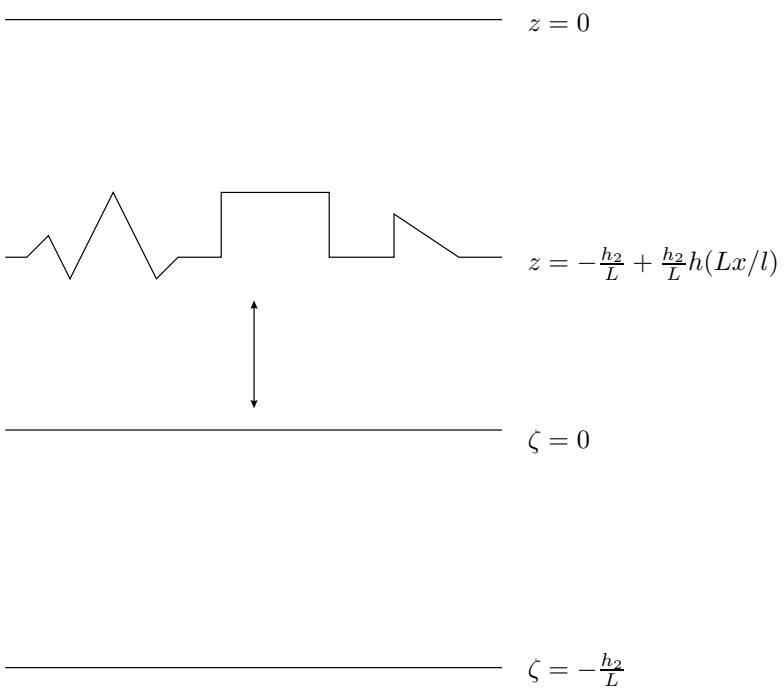

FIG. 2.2. *Conformal mapping,* $(x,z)=\big(\mathrm{x}(\xi,\zeta),\mathrm{z}(\xi,\zeta)\big)$.

and therefore,

$$\phi_z(x,0,t)=\eta_t+O\left(\sqrt{\beta}\right).$$

To find the horizontal velocity $\phi_x(x,0,t)$ in problem (2.16), a conformal mapping between the flat strip $\zeta\in\left[-\frac{h_2}{L},0\right]$ and the lower layer at rest is performed. See Fig. 2.2.

The problem in conformal coordinates is

$$\begin{cases} \phi_{\xi\xi}+\phi_{\zeta\zeta}=0, & \text{on } -\dfrac{h_2}{L}\le\zeta\le 0,\\ \phi_\zeta(\xi,0,t)=M(\xi)\,\eta_t\big(\mathrm{x}(\xi,0),t\big), & \text{at } \zeta=0,\\ \phi_\zeta=0, & \text{at } \zeta=-\dfrac{h_2}{L}, \end{cases} \tag{2.17}$$

where the previous Neumann condition at the top is now modified by $M(\xi)=\mathrm{z}_\zeta(\xi,0)$ which is the nonzero element of the Jacobian of the conformal mapping at the unperturbed interface. As shown in [24], its exact expression is

$$M(\xi_0)=1-\frac{\pi}{4}\frac{L}{h_2}\int_{-\infty}^{\infty}\frac{h\big(L\mathrm{x}(\xi,-h_2/L)/l\big)}{\cosh^2\left(\frac{\pi L}{2h_2}(\xi-\xi_0)\right)}d\xi.$$

Moreover, the Jacobian along the unperturbed interface is an analytic function.

Hence a highly complex boundary profile has been converted into a smooth variable coefficient in the equations.

Since a conformal mapping was used in the coordinate transformation and $\mathrm{z}_\xi(\xi,0)=0$, it is guaranteed that $\mathrm{z}_\zeta(\xi,0)=\mathrm{x}_\xi(\xi,0)$ is different from zero. From $\phi_\xi(\xi,0,t)=\phi_x(x,0,t)\mathrm{x}_\xi(\xi,0)$, the velocity $\phi_x(x,0,t)$ is recovered as

$$\phi_x(x,0,t)=\frac{\phi_\xi(\xi,0,t)}{M(\xi)}.$$

The bottom Neumann condition is trivial in these new coordinates.

Notice that the terrain-following velocity component $\phi_\xi(\xi,0,t)$ is a tangential derivative on the boundary for problem (2.17). Hence it can be obtained as the Hilbert transform on the strip (see [17]) applied to the Neumann data. Namely

$$\phi_\xi(\xi,0,t)=\mathcal{T}\left[M(\tilde{\xi})\eta_t\big(\mathrm{x}(\tilde{\xi},0),t\big)\right](\xi),$$

where

$$\mathcal{T}[f](\xi)=\frac{1}{2h}\fint f(\tilde{\xi})\coth\Big(\frac{\pi}{2h}(\tilde{\xi}-\xi)\Big)\,d\tilde{\xi} \tag{2.18}$$

is the Hilbert transform on the strip of height h. In this case, $h=h_2/L$. The singular integral must be interpreted as a Cauchy principal value. The effect of the two-dimensional undisturbed layer below the interface is being collapsed onto a one-dimensional singular integral without any approximation. The results above are used in (2.15) by noting that ϕ_{tx} is obtained after taking the time derivative of problem (2.16).

Finally, substituting the expression for P_x in the upper layer averaged equations gives

$$\begin{cases}\eta_t-\big[(1-\eta)\overline{u_1}\big]_x=0,\\ \overline{u_1}_t+\overline{u_1}\,\overline{u_1}_x+\left(1-\dfrac{\rho_2}{\rho_1}\right)\eta_x=\\ \quad\sqrt{\beta}\dfrac{L}{2h_2}\dfrac{\rho_2}{\rho_1}\dfrac{1}{M\big(\xi(x,0)\big)}\fint M(\tilde{\xi})\eta_{tt}\big(\mathrm{x}(\tilde{\xi},0),t\big)\coth\left(\dfrac{\pi L}{2h_2}\big(\tilde{\xi}-\xi(x,0)\big)\right)d\tilde{\xi}+O(\beta).\end{cases}$$

It remains to make a few manipulations with this set of equations: eliminate the second order (in time) derivative and write all spatial derivatives in the ξ-variable.

Note that the first equation is exact. According to it $\eta_{tt}=\big((1-\eta)\overline{u_1}\big)_{xt}$ so only the first time derivative of $\overline{u_1}$ needs to enter the right-hand side of the second equation.

In conclusion, the reduced one-dimensional internal wave model is:

$$\begin{cases}\eta_t-\big[(1-\eta)\overline{u_1}\big]_x=0,\\ \overline{u_1}_t+\overline{u_1}\,\overline{u_1}_x+\left(1-\dfrac{\rho_2}{\rho_1}\right)\eta_x=\sqrt{\beta}\dfrac{\rho_2}{\rho_1}\dfrac{1}{M(\xi)}\mathcal{T}\left[M(\cdot)\big((1-\eta)\overline{u_1}\big)_{xt}\big(\mathrm{x}(\cdot,0),t\big)\right],\end{cases} \tag{2.19}$$

where the dot indicates the variable on which the operator $\mathcal{T}$ is applied.

The transform in the forcing term is in curvilinear coordinates. For practical purposes both sides must be in the same coordinate system, which is readily adjusted

via the conformal mapping: every x-derivative is equal to a ξ-derivative divided by the Jacobian $M(\xi)$. Therefore, system (2.19) in the terrain-following coordinates reads

$$\begin{cases} \eta_t - \dfrac{1}{M(\xi)}\left[(1-\eta)\overline{u_1}\right]_\xi = 0, \\ \overline{u_1}_t + \dfrac{1}{M(\xi)}\overline{u_1}\,\overline{u_1}_\xi + \dfrac{1}{M(\xi)}\left(1-\dfrac{\rho_2}{\rho_1}\right)\eta_\xi = \sqrt{\beta}\,\dfrac{\rho_2}{\rho_1}\dfrac{1}{M(\xi)}\mathcal{T}\left[\left((1-\eta)\overline{u_1}\right)_{\xi t}\right]. \end{cases} \tag{2.20}$$

This is a Boussinesq-type system with variable (time independent) coefficients depending on $M(\xi)$ for the perturbation of the interface η and the mean (upper-layer) horizontal velocity $\overline{u_1}$. As will be shown below this is a dispersive model, where the dispersion term comes in through the Hilbert transform. Since no smallness assumption was made on the wave amplitude up to now, the model derived is strongly nonlinear. It involves a Hilbert transform on the strip characterizing the presence of harmonic functions (hence the potential flow) below the interface. Efficient computational methods can be produced for this accurate reduced model which governs, to leading order, a complex two-dimensional problem. A brief description of these methods is given below.

If the bottom is flat, $M(\xi)=1$ and the same system derived in [7] is obtained, which is a nice consistency check.

When the lower depth tends to infinity ($h_2 \to \infty$) the limit for this model is the same one obtained in [7] because the bottom is not seen anymore ($M(\xi)\to 1$ and $\mathrm{x}(\tilde{\xi},0)\to\tilde{\xi}$). Therefore

$$\phi_{xt}(x,0,t) \to \frac{1}{\pi}\int \frac{\left((1-\eta)\overline{u_1}\right)_{xt}(\tilde{x},t)}{\tilde{x}-x}\,d\tilde{x} = \mathcal{H}\left[\left((1-\eta)\overline{u_1}\right)_{xt}\right](x),$$

where $\mathcal{H}$ is the usual Hilbert transform defined as

$$\mathcal{H}[f](x) = \frac{1}{\pi}\int \frac{f(\tilde{x})}{\tilde{x}-x}\,d\tilde{x}.$$

In this (shallow upper layer) infinite lower layer regime, system (2.19) becomes

$$\begin{cases} \eta_t - \left[(1-\eta)\overline{u_1}\right]_x = 0, \\ \overline{u_1}_t + \overline{u_1}\,\overline{u_1}_x + \left(1-\dfrac{\rho_2}{\rho_1}\right)\eta_x = \sqrt{\beta}\dfrac{\rho_2}{\rho_1}\mathcal{H}\left[\left((1-\eta)\overline{u_1}\right)_{xt}\right]. \end{cases} \tag{2.21}$$

Later on in this work we will comment on how the regularized Benjamin–Ono equation arises from the unidirectional wave regime of the above system.

3. A brief discussion on numerical modeling

The Fourier Transform (FT) of a Hilbert transform is easily computed. We now make a comment regarding the use of DFTs in numerical schemes. Both operators $\mathcal{T}[f]$ and $\mathcal{H}[f]$ have Fourier transforms of the form

$$\widehat{\mathcal{T}[f]} = i\coth\left(\frac{kh_2}{L}\right)\hat{f},$$
$$\widehat{\mathcal{H}[f]} = i\,\mathrm{sgn}(k)\hat{f},$$

where the operator's symbol multiplies the transform of f, namely $\hat{f}$. Therefore in Eqs. (2.20) and (2.21) a pseudospectral scheme would apply a DFT to the terms inside

the square brackets. FFTs are only aplicable directly when $M(\xi)=1$ and the waves are weakly nonlinear.

For the flat bottom version of system (2.20), Choi and Camassa in [7] used a pseudospectral method in space. Then they combined the time derivatives in the second equation to make the evolution in time for η and V, where $V=\overline{u_1}-\sqrt{\beta}\frac{\rho_2}{\rho_1}\mathcal{T}\left[\left((1-\eta)\overline{u_1}\right)_\xi\right]$. The time evolution was performed by a fourth order Runge-Kutta integration scheme. To recover $\overline{u_1}$ after each evolution step, an algebraic equation was solved involving the spectral differentiation matrix for the spatial derivative (namely via a DFT procedure) and the convolution matrix for the operator $\mathcal{T}$. Since model (2.20) differs only in a variable time independent coefficient, this numerical formulation applies. The coefficient $M(\xi)$ at the grid points is computed just once for a given topography by using Driscoll's package [9].

In [27] and [23], a similar numerical solver was applied to two different nonlinear Boussinesq systems. Instead of spectral differentiation, they used a fourth order finite difference approximation for the spatial derivatives. For the evolution in time a predictor-corrector method combining a third order, three step Adams-Bashforth scheme and a fourth order, three step Adams-Moulton scheme was implemented. With these choices all truncation errors were reduced to a level smaller than the dispersive terms retained by their models. Accurate results were observed including experiments for solitary waves over highly disordered topographies.

The three step Adams-Moulton scheme has a smaller stability interval along the imaginary axis (where the eigenvalues of the linearized spatial discretization operators lie) than the fourth order Runge-Kutta scheme. This implies a stronger restriction to avoid instabilities when using the Adams-Moulton scheme to solve the bidirectional wave equation, for example. We have compared these two strategies for the terrain-following system in [23] and noticed that with a Runge-Kutta scheme we can use larger time steps. However, for the regularized systems considered here we got better results (less instability) since the phase velocity actually decreases as the wave number grows, hence accommodating high wave-numbers better than in the hyperbolic case. Dispersion relations are given below. Still, the classical fourth order Runge-Kutta seems to be a better choice.

Results for the computational methods available (and partially described here) will be published elsewhere in the near future. These will include experiments over random topography as those presented in [13, 22, 10, 25, 14] for the apparent diffusion and [23, 12, 10, 11] for time-reversal refocusing of waves.

The dispersion relation for the flat bottom case ($M(\xi)=1$) is the same one obtained in [7]:

$$\omega^2=\frac{\left(\frac{\rho_2}{\rho_1}-1\right)k^2}{1+\frac{\rho_2}{\rho_1}k\sqrt{\beta}\coth\left(\frac{kh_2}{L}\right)}, \tag{3.1}$$

is the correct approximation to the full dispersion relation that comes from the linearized Euler equations around the undisturbed state, [19]. Namely arising from

$$\omega^2=\frac{\left(\frac{\rho_2}{\rho_1}-1\right)k^2}{\frac{kh_1}{L}\coth\left(\frac{kh_1}{L}\right)+\frac{\rho_2}{\rho_1}k\sqrt{\beta}\coth\left(\frac{kh_2}{L}\right)},$$

when kh_1 is near zero. A nonvanishing value of the parameter β in the dispersion relation (3.1) makes the phase velocity a function of the wave number k. Observe

that $\frac{\omega^2}{k^2} \to 0$ as $k \to \infty$, so bounded phase velocities are obtained as k becomes large. This is a good property for numerical schemes.

The dispersion relation for system (2.21) is

$$\omega^2 = \frac{\left(\frac{\rho_2}{\rho_1} - 1\right) k^2}{1 + \frac{\rho_2}{\rho_1} |k| \sqrt{\beta}}$$

and $\frac{\omega^2}{k^2} \to 0$ as $k \to \infty$.

4. Unidirectional wave regime

For weakly nonlinear unidirectional waves and slowly varying topography, our model reduces to a single ILW equation with variable coefficients.

Consider again system (2.19), except for the Jacobian of the conformal mapping which now is

$$M(\xi_0) = 1 - \frac{\pi}{4} \frac{L}{h_2} \int_{-\infty}^{\infty} \frac{h\big(\varepsilon \mathrm{x}(\xi, -h_2/L)\big)}{\cosh^2\left(\frac{\pi L}{2h_2}(\xi - \xi_0)\right)} d\xi,$$

since we assume a slowly varying bottom topography described in non-dimensional coordinates as $z = -\frac{h_2}{L} + \frac{h_2}{L} h(\varepsilon x)$, with $\varepsilon \ll 1$. The restriction to a slowly varying topography is consistent with the objective of the present section, which is to find equations to model the unidirectional wave propagation. Hence there will be no reflection nor any backward evolution opposite to the propagation direction.

To study the weakly nonlinear regime, introduce the typical amplitude a for the perturbation of the interface and introduce the nonlinearity parameter $\alpha = \frac{a}{h_1}$ of order $O\left(\sqrt{\beta}\right)$. As usual in a weakly nonlinear theory, set $\eta = \alpha \eta^*$. With this, the original dimensional perturbation η is nondimensionalized as $\eta = \alpha h_1 \eta^* = a\eta^*$. Say also that $\overline{u_1} = \alpha c_0 \overline{u_1}^*$, $t = \frac{t^*}{c_0}$ where $c_0^2 = \left(\frac{\rho_2}{\rho_1} - 1\right)$. Depending on the root c_0 chosen, there will be a right- or left-travelling wave.

Then, dropping the asterisks, we have

$$\begin{cases} \eta_t - \left[(1 - \alpha\eta)\overline{u_1}\right]_x = 0, \\ \overline{u_1}_t + \alpha \overline{u_1}\,\overline{u_1}_x - \eta_x = \sqrt{\beta} \dfrac{\rho_2}{\rho_1} \dfrac{1}{M(\xi)} \mathcal{T}\left[M(\tilde{\xi})\left[(1 - \alpha\eta)\overline{u_1}\right]_{xt}\right] + O(\beta). \end{cases} \tag{4.1}$$

Note that

$$\eta_t = \overline{u_1}_x + O(\alpha); \qquad \eta_x = \overline{u_1}_t + O\left(\alpha, \sqrt{\beta}\right). \tag{4.2}$$

As in [7], look for a solution, up to a first order correction in α and $\sqrt{\beta}$, in the form

$$\eta = A_1 \overline{u_1} + \alpha A_2 \overline{u_1}^2 + \sqrt{\beta} A_3 \frac{1}{M(\xi)} \mathcal{T}\left[M(\tilde{\xi}) \overline{u_1}_t\right], \tag{4.3}$$

with coefficients A_i to be determined. Substituting in the system of Eqs. (4.1) up to order α, $\sqrt{\beta}$, two equations for $\overline{u_1}$ are obtained:

$$0 = A_1 \overline{u_1}_t + 2\alpha A_2 \overline{u_1}\,\overline{u_1}_t + 2\alpha A_1 \overline{u_1}\,\overline{u_1}_x - \overline{u_1}_x + \sqrt{\beta} A_3 \frac{1}{M(\xi)} \mathcal{T}\left[M(\tilde{\xi}) \overline{u_1}_{tt}\right]$$

and

$$0=\overline{u_1}_t+\alpha\overline{u_1}\,\overline{u_1}_x-\left[A_1\overline{u_1}_x+2\alpha A_2\overline{u_1}\,\overline{u_1}_x+\sqrt{\beta}A_3\frac{1}{M(\xi)}\mathcal{T}\left[M(\tilde{\xi})\overline{u_1}_{xt}\right]\right]-$$
$$-\sqrt{\beta}\frac{\rho_2}{\rho_1}\frac{1}{M(\xi)}\mathcal{T}\left[M(\tilde{\xi})\overline{u_1}_{xt}\right]+O\left(\alpha^2,\beta,\alpha\sqrt{\beta}\right).$$

For compatibility and the choice of a right-going wave we let $A_1=-1$. Therefore

$$\eta_x=-\overline{u_1}_x+O\left(\alpha,\sqrt{\beta}\right), \tag{4.4}$$

so $\overline{u_1}_t=-\overline{u_1}_x+O\left(\alpha,\sqrt{\beta}\right)$ and $\overline{u_1}_{tt}=-\overline{u_1}_{xt}+O\left(\alpha,\sqrt{\beta}\right)$ and the two equations are consistent if $A_1=-1$, $A_2=-\frac{1}{4}$ and $A_3=-\frac{\rho_2}{2\rho_1}$. As a result, the evolution equation for $\overline{u_1}$ is

$$\overline{u_1}_t+\frac{3}{2}\alpha\overline{u_1}\,\overline{u_1}_x+\overline{u_1}_x-\frac{\rho_2}{\rho_1}\frac{\sqrt{\beta}}{2}\frac{1}{M(\xi)}\mathcal{T}\left[M(\tilde{\xi})\overline{u_1}_{xt}\right]=O\left(\beta,\alpha^2,\alpha\sqrt{\beta}\right).$$

For the elevation of the interface η a similar equation can be obtained through asymptotic relations which permit (to leading order) exchange derivatives in η for derivatives in $\overline{u_1}$, as well as time derivatives for spatial derivatives. This is a consequence of (4.3). To begin with, use

$$\overline{u_1}_{xt}=-\eta_{xt}+O\left(\alpha,\sqrt{\beta}\right)$$

so that

$$\frac{\sqrt{\beta}}{2}\frac{\rho_2}{\rho_1}\frac{1}{M(\xi)}\mathcal{T}\left[M(\tilde{\xi})\overline{u_1}_{xt}\right]=-\frac{\sqrt{\beta}}{2}\frac{\rho_2}{\rho_1}\frac{1}{M(\xi)}\mathcal{T}\left[M(\tilde{\xi})\eta_{xt}\right]+O\left(\alpha^2,\beta,\alpha\sqrt{\beta}\right). \tag{4.5}$$

In virtue of Eqs. (4.4) and (4.3)

$$\begin{aligned}\frac{3}{2}\alpha\overline{u_1}\,\overline{u_1}_x&=\frac{3}{2}\alpha\left(-\eta_x+O\left(\alpha,\sqrt{\beta}\right)\right)\left(-\eta+O\left(\alpha,\sqrt{\beta}\right)\right),\\&=\frac{3}{2}\alpha\eta\eta_x+O\left(\alpha^2,\alpha\sqrt{\beta}\right),\end{aligned} \tag{4.6}$$

and for similar reasons

$$\begin{aligned}\eta_t+\eta_x&=-(\overline{u_1}_t+\overline{u_1}_x)-\frac{\alpha}{2}\overline{u_1}(\overline{u_1}_t+\overline{u_1}_x)-\frac{\sqrt{\beta}}{2}\frac{\rho_2}{\rho_1}\frac{1}{M(\xi)}\mathcal{T}\left[M(\tilde{\xi})(\overline{u_1}_{tt}+\overline{u_1}_{xt})\right],\\&=-(\overline{u_1}_t+\overline{u_1}_x)+O\left(\alpha^2,\alpha\sqrt{\beta},\beta\right).\end{aligned} \tag{4.7}$$

Substituting all these expressions in the evolution equation for $\overline{u_1}$ we obtain the evolution equation for the elevation of the interface,

$$\eta_t+\eta_x-\frac{3}{2}\alpha\eta\eta_x-\frac{\rho_2}{\rho_1}\frac{\sqrt{\beta}}{2}\frac{1}{M(\xi)}\mathcal{T}\left[M(\tilde{\xi})\eta_{xt}\right]=O\left(\beta,\alpha^2,\alpha\sqrt{\beta}\right).$$

Finally, in the curvilinear coordinates we have

$$\eta_t+\frac{1}{M(\xi)}\eta_\xi-\frac{3}{2}\frac{\alpha}{M(\xi)}\eta\eta_\xi-\frac{\rho_2}{\rho_1}\frac{\sqrt{\beta}}{2}\frac{1}{M(\xi)}\mathcal{T}[\eta_{\xi t}]=0. \tag{4.8}$$

This is an ILW equation with variable coefficients accounting for the slowly varying bottom topography. Instead of the usual Hilbert transform on the half-space, a Hilbert transform on the strip appears. The dispersion relation for the flat bottom case ($M(\xi)=1$) is

$$\omega = \frac{k}{1+\frac{\rho_2}{\rho_1}\frac{\sqrt{\beta}}{2}k\coth\left(\frac{kh_2}{L}\right)}. \tag{4.9}$$

The equation reduces to a regularized dispersive model in analogy with the Benjamin-Bona-Mahony equation (BBM) [3].

The constant coefficient version of Eq. (4.8) differs from the one deduced in [7] in that the latter has a dispersion term with only spatial derivatives as in the KdV equation. Both constant coefficient equations are equivalent up to the order considered since we can substitute $\eta_{\xi t}$ by $-\eta_{\xi\xi}$ in the dispersion term up to order $O\left(\beta,\alpha\sqrt{\beta}\right)$. There are two advantages for our choice. First, for every change from a Cartesian x-derivative to a curvilinear ξ-derivative we need the presence of the metric term $M(\xi)$. Hence for the Camassa-Choi model with the second order x-derivative we would end up with a variable coefficient within the nonlocal operator. Second, the regularized dispersive operator (namely with an xt-derivative) leads to the stable dispersion relation (4.9) regarding numerical schemes. Short waves have bounded propagation speeds. This does not happen with the ILW equation consider in [7], whose dispersion relation is

$$\omega = k - \frac{\rho_2}{\rho_1}\frac{\sqrt{\beta}}{2}k^2\coth\left(\frac{kh_2}{L}\right).$$

One step remains to be explained in the substitution of Eq. (4.3) into the second equation of system (4.1), namely why it is valid (for a slowly varying topography) that

$$\left(\frac{\sqrt{\beta}}{M(\xi)}\mathcal{T}\left[M(\tilde{\xi})\overline{u_1}_t\right]\right)_x = \frac{\sqrt{\beta}}{M(\xi)}\mathcal{T}\left[M(\tilde{\xi})\overline{u_1}_{tx}\right]+O(\beta). \tag{4.10}$$

This approximation was not presented in [7] since the present work contains for the first time the conformal mapping technique used for the lower layer. The approximation (4.10) is justified through the construction of an auxiliary PDE problem. See Appendix A for details.

For system (2.21) a similar unidirectional reduction can be obtained leading to

$$\eta_t+\eta_x-\frac{3}{2}\alpha\eta\eta_x-\frac{\rho_2}{\rho_1}\frac{\sqrt{\beta}}{2}\mathcal{H}[\eta_{xt}]=0,$$

which is a regularized Benjamin-Ono (BO) equation over an infinite bottom layer. Hence Eq. (4.8) is a generalization of the BO equation for intermediate depths and the presence of a topography. This equation is only valid when backscattering is negligible.

Conclusions. A one-dimensional variable coefficient Boussinesq-type model for the evolution of internal waves in a two-layer system is derived. The regime considered is a shallow water configuration for the upper layer and an intermediate depth for the lower layer. The bottom has an arbitrary, not necessarily smooth nor single-valued, profile generalizing the flat bottom model derived in [7]. This arbitrary topography

is dealt with by performing a conformal mapping as in [24]. In the unidirectional propagation regime the model reduces to an ILW equation when a slowly varying topography is assumed.

The adjustment for the periodic wave case as well as its computational implementation is relatively straightforward and will be published elsewhere together with detailed numerical experiments. We intend to use this model to study the interaction of internal waves with different types of bottom profiles such as submerged structures and multiscale topography profiles. As in [23, 21] stability analysis for the hyperbolic and weakly dispersive regimes are also of interest.

Models with a higher order pressure approximation are the objective of ongoing research and also of future numerical experimentation with solitary waves over a disordered topography.

Acknowledgements. The authors would like to thank Prof. W. Choi for his useful comments regarding this work and future extensions, and Prof. U. Ascher for his observations about the stability of numerical schemes.

Appendix A. Approximation for the horizontal derivatives at the unperturbed interface.

We want to justify the use of $\frac{\sqrt{\beta}}{M(\xi)}\mathcal{T}\left[M(\tilde{\xi})\overline{u_1}_{tx}\right]$ instead of $\left(\frac{\sqrt{\beta}}{M(\xi)}\mathcal{T}\left[M(\tilde{\xi})\overline{u_1}_{t}\right]\right)_x$ in the substitution of η_x in system (4.1), in the case of slowly varying topography. Hence we identify $\frac{1}{M(\xi)}\mathcal{T}\left[M(\tilde{\xi})\overline{u_1}_{t}\right]$ as the tangential derivative of the solution of the Laplace equation with Neumann conditions defined in the auxiliary problem

$$\begin{cases} \Phi_{xx}+\Phi_{zz}=0, & \text{on } -\dfrac{h_2}{L}+\dfrac{h_2}{L}h(\varepsilon x)\le z\le 0,\\[2ex] \Phi_z=\overline{u_1}_t, & \text{at } z=0,\\[2ex] \Phi_z-\varepsilon\dfrac{h_2}{L}h'(\varepsilon x)\Phi_x=0, & \text{at } z=-\dfrac{h_2}{L}+\dfrac{h_2}{L}h(\varepsilon x), \end{cases} \tag{A.1}$$

where ε is the small parameter defined at the beginning of the paper as L/l. It was already shown that

$$\Phi_x(x,0,t)=\frac{1}{M(\xi)}\mathcal{T}\left[M(\tilde{\xi})\overline{u_1}_t\right]$$

via conformal mapping. Now we seek an approximation of $\Phi_{xx}(x,0,t)$, our term of interest, where t is kept frozen. Let $\omega(x,z)=\Phi_x(x,z,t)$. The tangential derivative of ω at $z=0$ is our goal. From Eqs. (A.1), ω satisfies

$$\begin{cases} \omega_{xx}+\omega_{zz}=0, & \text{on } -\dfrac{h_2}{L}+\dfrac{h_2}{L}h(\varepsilon x)\le z\le 0,\\[2ex] \omega_z=\overline{u_1}_{xt}, & \text{at } z=0,\\[2ex] \omega_z-\varepsilon\dfrac{h_2}{L}h'(\varepsilon x)\omega_x-\varepsilon^2\dfrac{h_2}{L}h''(\varepsilon x)\omega=0, & \text{at } z=-\dfrac{h_2}{L}+\dfrac{h_2}{L}h(\varepsilon x). \end{cases}$$

A conformal mapping taking a flat strip into the corrugated strip above transforms

this problem into

$$\begin{cases} \omega_{\xi\xi}+\omega_{\zeta\zeta}=0, & \text{on } -\dfrac{h_2}{L}\le\zeta\le 0,\\ \omega_\zeta = M(\xi)\overline{u_1}_{xt}\big(\mathrm{x}(\xi,0),t\big), & \text{at } \zeta=0,\\ \omega_\zeta-\varepsilon^2\dfrac{h_2}{L}h''\big(\varepsilon\mathrm{x}(\xi,0)\big)\omega=0, & \text{at } \zeta=-\dfrac{h_2}{L}. \end{cases}$$

Note that a mixed boundary condition (Robin condition) is set on $\zeta=-\frac{h_2}{L}$ instead of a Neumann condition as in all previous problems. Because of the Robin condition, the tangential derivative $\omega_\xi(\xi,0,t)$ is no longer $\mathcal{T}\left[M(\tilde{\xi})\overline{u_1}_{xt}\big(\mathrm{x}(\tilde{\xi},0),t\big)\right]$, but it can be approximated by this term up to a certain order in ε. Following a perturbation approach, consider

$$\omega=\omega_0+\varepsilon\omega_1+\varepsilon^2\omega_2+\cdots$$

then ω_0 satisfies the Neumann problem

$$\begin{cases} \omega_{0\xi\xi}+\omega_{0\zeta\zeta}=0, & \text{on } -\dfrac{h_2}{L}\le\zeta\le 0,\\ \omega_{0\zeta}=M(\xi)\overline{u_1}_{xt}\big(\mathrm{x}(\xi,0),t\big), & \text{at } \zeta=0,\\ \omega_{0\zeta}=0, & \text{at } \zeta=-\dfrac{h_2}{L}, \end{cases}$$

with tangential derivative $\omega_{0\xi}(\xi,0)=\mathcal{T}\left[M(\tilde{\xi})\overline{u_1}_{xt}\big(\mathrm{x}(\tilde{\xi},0),t\big)\right](\xi)$. Thus $\omega_{0x}=\omega_{0\xi}/M(\xi)$. The subsequent term is $\omega_1=0$ because both boundary conditions are homogeneous to $O(\varepsilon)$. Next ω_2 satisfies

$$\begin{cases} \omega_{2\xi\xi}+\omega_{2\zeta\zeta}=0, & \text{on } -\dfrac{h_2}{L}\le\zeta\le 0,\\ \omega_{2\zeta}=0, & \text{at } \zeta=0,\\ \omega_{2\zeta}-\dfrac{h_2}{L}h''\big(\varepsilon\mathrm{x}(\xi,0)\big)\omega_0=0, & \text{at } \zeta=-\dfrac{h_2}{L}. \end{cases}$$

Therefore

$$\omega=\omega_0+O(\varepsilon^2). \tag{A.2}$$

If we establish a relation between α, β and ε of the type $\varepsilon^2=O(\beta^q)$, with $q\ge\frac{1}{2}$, Eq. (A.2) leads to

$$\left(\frac{1}{M(\xi)}\mathcal{T}\left[M(\tilde{\xi})\overline{u_1}_t\right]\right)_x=\frac{1}{M(\xi)}\mathcal{T}\left[M(\tilde{\xi})\overline{u_1}_{tx}\right]+O\left(\sqrt{\beta}\right),$$

which justifies the approximation done in Eq. (4.10).

REFERENCES

[1] W. Artiles and A. Nachbin, *Nonlinear evolution of surface gravity waves over highly variable depth*, Physical Review Letters, vol. 93, pp. 234501-1–234501-4, 2004.

[2] T. B. Benjamin, *Internal waves of permanent form of great depth*, Journal of Fluid Mechanics, vol. 29, pp. 559–592, 1967.

[3] T. B. Benjamin, J. L. Bona, J. J. Mahony, *Model equations for long waves in nonlinear dispersive systems*, Philosophical Transactions of the Royal Society of London. Series A, Mathematical and Physical Sciences, vol. 272, No. 1220, pp. 47–78, 1972.

[4] R. Camassa and C. D. Levermore, *Layer-mean quantities, local conservation laws, and vorticity*, Physical Review Letters, vol. 78, pp. 650–653, 1997.

[5] W. Choi and R. Camassa, *Long internal waves of finite amplitude*, Physical Review Letters, vol. 77, pp. 1759–1762, 1996.

[6] W. Choi and R. Camassa, *Weakly nonlinear internal waves in a two-fluid system*, Journal of Fluid Mechanics, vol. 313, pp. 83–103, 1996.

[7] W. Choi and R. Camassa, *Fully nonlinear internal waves in a two-fluid system*, Journal of Fluid Mechanics, vol. 396, pp. 1–36, 1999.

[8] R. E. Davis and A. Acrivos, *Solitary internal waves in deep water*, Journal of Fluid Mechanics, vol. 29, pp. 593–607, 1967.

[9] T. Driscoll, *Schwarz-Christoffel toolbox for* Matlab, http://www.math.udel.edu/driscoll/software.

[10] J. P. Fouque, J. Garnier and A. Nachbin, *Shock structure due to stochastic forcing and the time reversal of nonlinear waves*, Physica D, vol. 195, pp. 324–346, 2004.

[11] J. P. Fouque, J. Garnier and A. Nachbin, *Time reversal for dispersive waves in random media*, SIAM Journal of Applied Mathematics, vol. 64, issue. 5, pp. 1810–1838, 2004.

[12] J. P. Fouque, J. Garnier, J. C. Muñoz and A. Nachbin, *Time reversing solitary waves*, Physical Review Letters, vol. 92, No. 9, 094502-1, 2004.

[13] J. Garnier and A. Nachbin, *The eddy viscosity for time reversing waves in a dissipative environment*, Physical Review Letters, vol. 93, No. 15, 154501, 2004.

[14] J. Garnier and A. Nachbin, *The eddy viscosity for gravity waves propagating over turbulent surfaces*, Physics of Fluids, vol. 18, 055101, 2006.

[15] T.-C. Jo and W. Choi, *Dynamics of strongly nonlinear internal solitary waves in shallow water*, Studies in Applied Mathematics, vol. 109, pp. 205–227, 2002.

[16] R. I. Joseph, *Solitary waves in finite depth fluid*, Journal of Physics *A*, vol. 10, pp. L225–L227, 1977.

[17] J. P. Keener, *Principles of Applied Mathematics: Transformation and Approximation*, Westview Press, 2000.

[18] T. Kubota, D. Ko and L. Dobbs, *Propagation of weakly nonlinear internal waves in a stratified fluid of finite depth*, AIAA Journal Hydrodynamics, vol. 12, pp. 157–165, 1978.

[19] H. Lamb, *Hydrodynamics*, Dover, 1932.

[20] Y. Matsuno, *A unified theory of nonlinear wave propagation in two-fluid systems*, Journal of the Physical Society of Japan, vol. 62, pp. 1902–1916, 1993.

[21] P. Milewski, E. Tabak, C. Turner, R. Rosales and F. Menzaque, *Nonlinear stability of two-layer flows*, Communications in Mathematical Sciences, vol. 2, No. 3, pp. 427–442, 2004.

[22] J. C. Muñoz and A. Nachbin, *Dispersive wave attenuation due to orographic forcing*, SIAM Journal of Applied Mathematics, vol. 64, Issue 3, pp. 977–1001, 2004.

[23] J. C. Muñoz and A. Nachbin, *Stiff microscale forcing and solitary wave refocusing*, SIAM Multiscale Modeling and Simulation, vol. 3, issue 3, pp. 680–705, 2005.

[24] A. Nachbin, *A terrain-following Boussinesq system*, SIAM Journal on Applied Mathematics, vol. 63, pp. 905–922, 2003.

[25] A. Nachbin and K. Solna, *Apparent diffusion due to orographic microstructure in shallow waters*, Physics of Fluids, vol. 15, No. 1, pp. 66–77, 2003.

[26] H. Ono, *Algebraic solitary waves in stratified fluids*, Journal of the Physical Society of Japan, vol. 39, pp. 1082–1091, 1975.

[27] G. Wei and J. Kirby, *Time-dependent numerical code for extended Boussinesq equations*, Journal of Waterway, Port, Coastal and Ocean Engineering, vol. 121 pp. 251–261, 1995.

[28] T. Y. Wu, *Long waves in ocean and coastal waters*, Journal of the Engineering Mechanics Division ASCE, vol. 107, No. 3, pp. 501–522, 1981.